ScientificScholar®
Knowledge is power
Publisher of Scientific Journals

www.surgicalneurologyint.com

Surgical Neurology International

Editor-in-Chief: Nancy E. Epstein, MD, Clinical Professor of Neurological Surgery, School of Medicine, State U. of NY at Stony Brook.

SNI: Neuroanatomy and Neurophysiology

Editor
Seyed Ali Khonsary, MD
University of California at Los Angeles, Los Angeles, CA, USA

SNI
Open Access

Original Article

Changes in vascular supply pattern associated with growth of nonfunctioning pituitary adenomas

Miiko Ito[1], Yuta Mitobe[1], Toshitada Hiraka[2], Masafumi Kanoto[2], Yukihiko Sonoda[1]

[1]Department of Neurosurgery, Yamagata University, [2]Department of Diagnostic Radiology, Faculty of Medicine, Yamagata University, Yamagata, Japan.

E-mail: Miiko Ito - miiko0908@gmail.com; Yuta Mitobe - y-mitobe@med.id.yamagata-u.ac.jp; Toshitada Hiraka - hirakatoshitada@gmail.com; Masafumi Kanoto - mkanoto@med.id.yamagata-u.ac.jp; *Yukihiko Sonoda - yukihikosonoda@gmail.com

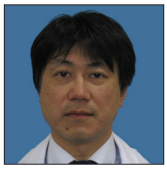

***Corresponding author:**
Yukihiko Sonoda,
Department of Neurosurgery,
Yamagata University, Yamagata,
Japan.

yukihikosonoda@gmail.com

Received : 21 September 2022
Accepted : 04 October 2022
Published : 21 October 2022

DOI
10.25259/SNI_879_2022

Quick Response Code:

ABSTRACT

Background: The vascular supply to nonfunctioning pituitary adenomas (NFPAs) differs compared with that of the anterior lobe of the normal pituitary gland. In this study, we aimed to identify feeding arteries and flow dynamics using 3.0 T magnetic resonance imaging (MRI) in NFPAs.

Methods: We divided 77 cases of NFPA into three groups according to the time-intensity curve (TIC) pattern by dynamic MRI. We also investigated the presence of feeder arteries as a flow void signal on T2-weighted imaging (T2WI).

Results: According to the TIC, 39 cases demonstrated an ascending pattern, 10 cases demonstrated a descending pattern, and 28 cases demonstrated a monophasic pattern. Tumor size in the ascending group was larger compared with the descending group ($P = 0.0036$). Flow void signals were identified in 51 of 77 cases (66.2%) on T2WI. Tumor size was larger in tumors with a flow void signal compared with those without ($P < 0.0001$). Flow void signals were more frequently observed in the group of ascending pattern compared with the group of monophasic and descending pattern ($P = 0.032$ and $P = 0.003$, respectively). Particularly on the caudal side, the difference between the ascending group and the monophasic and descending groups was remarkable ($P = 0.0035$ and $P < 0.0001$, respectively).

Conclusion: We successfully evaluated the blood supply pattern by the TIC analysis and identified flow voids using 3.0 T MRI. Blood supply pattern was significantly associated with NFPA size. These results suggested that NFPA hemodynamics changes during tumor growth.

Keywords: Anastomose, Blood supply, Dynamic study, Nonfunctioning pituitary adenoma, Time-intensity curve

INTRODUCTION

The vascular supply of pituitary adenomas (PA) is not well understood. Previously, we reported three blood supply patterns (descending, monophasic, and ascending) in nonfunctioning pituitary adenomas (NFPAs) by the time-intensity curve (TIC) analysis using pituitary dynamic magnetic resonance imaging (MRI).[8] With the descending pattern, blood supply mainly originates from the middle hypophyseal artery (MHA) branched from the superior hypophyseal artery (SHA). Conversely, tumors with an ascending pattern receive their vascular supply from vessels in the lower plane.

Recently, some papers reported that PA feeding arteries are visible as flow void signals on MRI.[9,14]

In this study, we aimed to identify feeding arteries and the blood supply pattern using 3.0 T MRI to determine the changes occurred during the process of growth in NFPAs.

MATERIALS AND METHODS

Patient selection

This retrospective study was conducted with the approval of the Ethics Committee of Yamagata University School of Medicine. Written informed consent was obtained from all patients before their participation in the study.

From July 2008 to December 2020, a total of 135 patients with NFPA underwent endoscopic transsphenoidal surgery (eTSS) at Yamagata University Hospital. All patients met the following inclusion criteria: (1) a diagnosis of NFPA; (2) no history of pituitary apoplexy; (3) undergoing a preoperative dynamic study; and (4) patients without large cystic formation in the tumor parenchyma on preoperative MRI. We analyzed a total of 77 patients with NFPA.

Radiological evaluation

All scans were performed using a 3.0 Tesla MRI unit (Discovery 750w, GE Healthcare, Milwaukee, Wisconsin) with a 24-channel head coil. The parameters for the plane MRI sequence are as follows: for sagittal T1-weighted TSE images, TR/TE of 400/12 ms, slice thickness of 3 mm without a gap, a matrix of 320 × 256, 180 × 180 mm FOV; for coronal T1-weighted TSE images, TR/TE of 437/12 ms, same as below; and for sagittal and coronal T2-weighted TSE images, TR/TE of 4000/80 ms, slice thickness of 3 mm without a gap, matrix of 320 × 224, 180 × 180 mm FOV. After precontrast sequence scanning, coronal dynamic contrast images were performed with rapid injection of a gadolinium-based contrast medium. Conventional coronal and sagittal postcontrast images were obtained with the following parameters: for dynamic coronal T1-weighted TSE images, TR/TE of 380/18 ms, three slices, dynamic scan in seven phases at 10, 26, 42, 57, 75, 100, and 130 s after injection, slice thickness of 3 mm with a gap of 0.5 mm, matrix of 288 × 160, 180 × 180 mm FOV; for sagittal postcontrast T1-weighted TSE image, TR/TE of 424/12 ms, slice thickness of 3 mm without a gap, matrix of 320 × 256, 180 × 180 mm FOV; and for coronal postcontrast T1-weighted TSE image, TR/TE of 516/12 ms, same as below.

As reported previously, we selected the section with the greatest longitudinal axis from among three slices of dynamic MRI scans and used it [Figure 1].[8] The long axis of the tumor was divided into two parts [Figure 1a]. For each component, we randomly chose three points in tumor parenchyma, calculated the mean signal intensity of the three points, and constructed a TIC. Intensity of the tumor increased rapidly in all cases and gradually decreased. TICs were classified into three patterns: descending, monophasic, and ascending pattern. The descending pattern was defined as that the time to peak intensity was shorter in the rostral section than in the caudal section, which indicated that blood was supplied in the rostral to caudal direction [Figure 1b]. Contrary to the descending pattern, in case of the ascending pattern, the time to peak intensity was shorter in the caudal section than in the rostral section [Figure 1d]. The monophasic pattern was defined as that there was no difference in the time to peak intensity between rostral and caudal sections [Figure 1c].

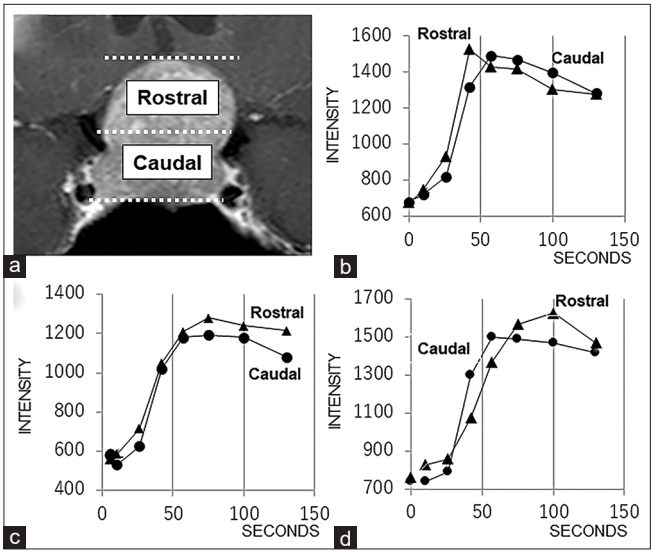

Figure 1: (a) The two components (rostral and caudal) used to evaluate blood supply patterns by time-intensity curve analysis. (b) A representative graph showing the descending hemodynamic pattern. (c) A representative graph showing the monophasic hemodynamic pattern. (d) A representative graph showing the ascending hemodynamic pattern.

We identified blood vessels as flow void signals on T2-weighted imaging (T2WI) [Figure 2] as previously reported.[9,14] Most of these flow void signals were consistent with intraoperative findings and required proper hemostasis. The location of flow void signals was classified into two parts (rostral and caudal), similar to the methods used in the TIC analysis [Figure 2].

Each neurosurgeon or neuroradiologist made initial evaluations individually, and consensus among them resolved any disagreements regarding final conclusions.

Statistical analysis

Data were analyzed using statistical software (Prism; GraphPad Software, capsular artery [CA]). The Kruskal–Wallis test was used to determine differences in tumor size among the three blood supply patterns in NFPAs. The relationship between two variables was evaluated using the Mann–Whitney U-test and Fisher's exact test. The significance level was set at $P < 0.05$.

RESULTS

The study included 77 patients (27 females and 50 males) with a median age of 63 years (range: 23–83 years). The median tumor size was 28 mm (range: 17–49 mm). According to the TIC classification, 10 cases demonstrated a descending pattern, 28 cases demonstrated a monophasic pattern, and 39 cases demonstrated an ascending pattern. There was a significant difference in tumor size among the three groups based on blood supply pattern ($P = 0.004$), [Figure 3a]. The size of tumors with an ascending pattern was significantly larger compared with those with a descending pattern ($P = 0.0036$) [Figure 3a]. The size of tumor with flow void signals was significantly larger compared to that without them ($P < 0.0001$) [Figure 3b]. Flow void signals were identified in 51 of 77 cases (66.2%) on T2WI [Figure 4a]. The signal was located rostrally in 18 cases (23.4%), caudally in 46 cases (59.7%), and on both sides in 14 cases (18.2%) [Figure 4]. The tumor size with flow void signals was 20–49 mm and without was 17–33 mm, respectively. Flow void signals were more frequently observed in tumors demonstrating the ascending pattern compared to them showing the descending pattern ($P = 0.032$ and $P = 0.003$, respectively), [Figure 4a]. There was a significant difference in the presence of a flow void at the rostral side between the group of monophasic pattern and the group of ascending pattern ($P = 0.038$), [Figure 4b]. Particularly on the caudal side, the difference between the group of ascending pattern and the group of monophasic or descending pattern was remarkable ($P = 0.0035$ and $P < 0.0001$, respectively), [Figure 4c]. Flow void signals at both sides were slightly more frequent in tumors with a monophasic pattern; however, there was no significant difference among the three groups of blood supply pattern [Figure 4d].

DISCUSSION

The normal pituitary gland was perfused from the superior (SHA) and inferior hypophyseal artery (IHA) branching from

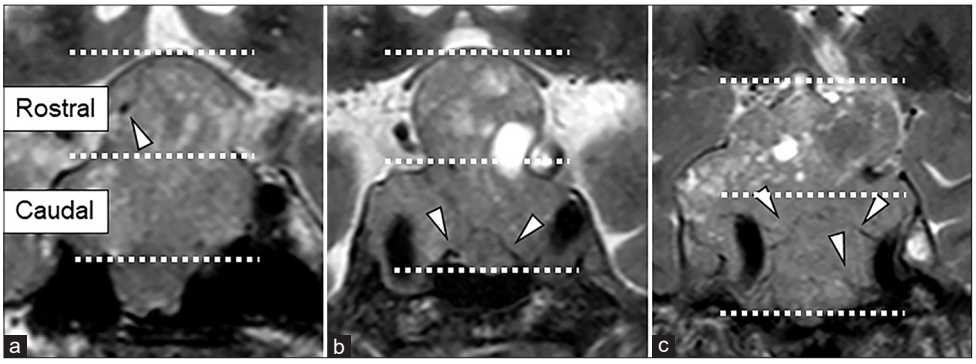

Figure 2: Preoperative 3.0 T magnetic resonance imaging (MRI) of coronal sections. T2-weighted imaging shows the tumor flow voids (a) at the rostral side, (b) at the caudal side in the basal plane, and (c) at the caudal side branching from the internal carotid artery. Arrow heads indicate flow voids.

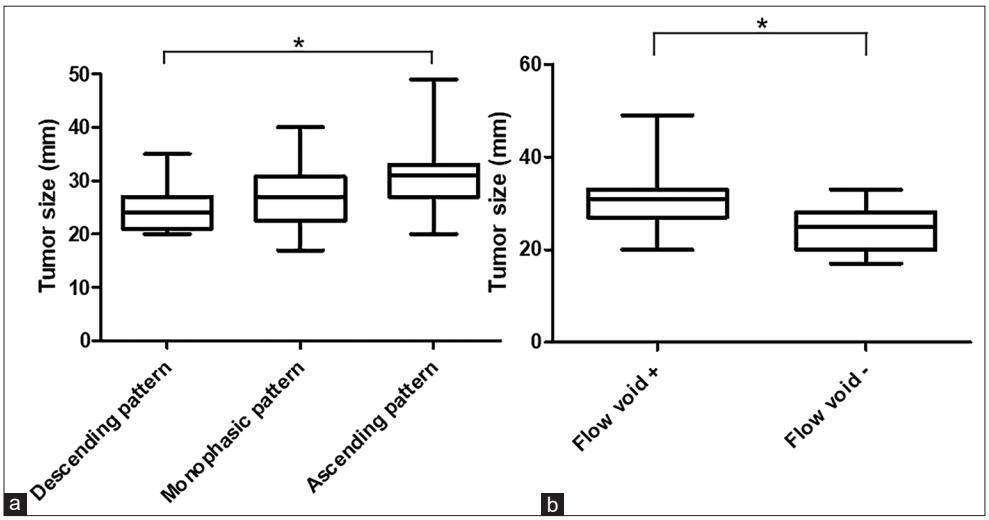

Figure 3: (a) Relationship between blood supply pattern and tumor size. (b) Relationship between presence of flow voids on MRI and tumor size. Asterisks indicate a significant difference.

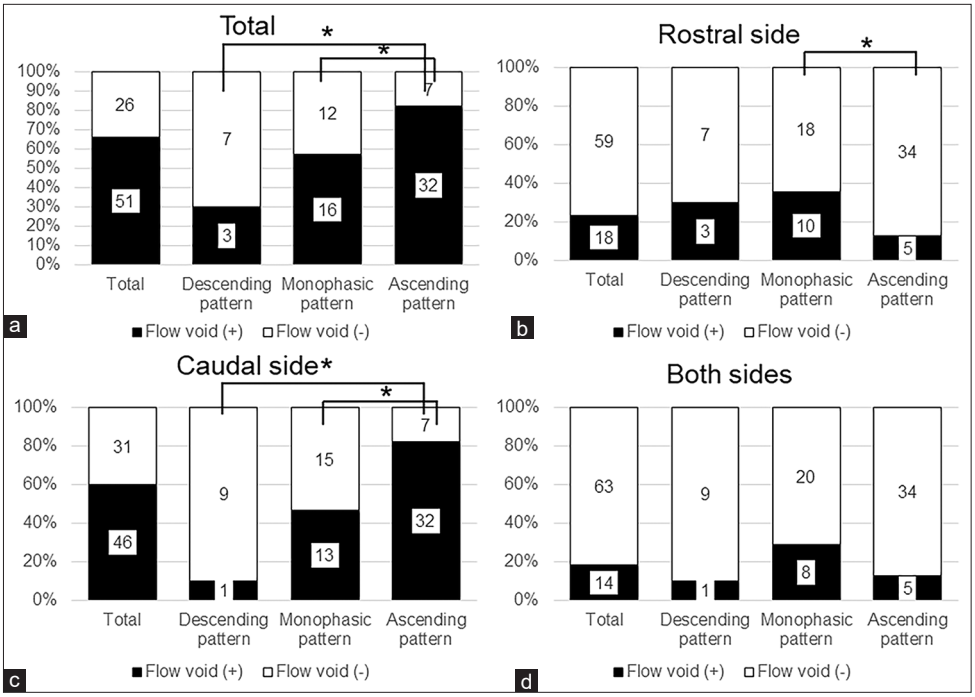

Figure 4: Difference in the presence of the flow void signal among groups according to blood supply pattern (a: total, b: rostral side, c: caudal side, d: both sides). Asterisks indicate a significant difference.

the internal carotid artery (ICA).[11] The SHA becomes the long portal vein and perfuses most of the anterior lobe and branches into the MHA. The MHA branches into the anterior fibrous core (AFC), perfusing the central part of the anterior lobe.[1,4,15,18,19] The base and ventral surfaces of the anterior lobe are perfused by the CA branching from the ICA.[6,12,15] The IHA is the maximal artery supplying the pituitary gland[10,12] directly into the posterior lobe and partially becomes a short portal vein perfusing the dorsal anterior lobe.[7,12] The IHA anastomoses between the left and right, also with inferior CA, and the arterial circle is formed at the base of the pituitary gland.[4,12] Furthermore, the SAH and IHA systems are anastomosed to each other[4,12,17,19] in many variations.[8]

Compared to the normal pituitary gland, which is mainly perfused by the portal vein, the blood supply of the PA was considered arterial. In autopsy cases, 66% of microadenomas had a direct extraportal arterial supply.[5] A dynamic CT study also showed that 34% of microadenomas had a partial or predominantly direct arterial blood supply.[3]

However, the normally invisible meningohypophyseal trunk (MHT) and CA were found angiographically in macroadenomas with suprasellar extension.[2] Powell *et al*. confirmed MHT in all macroadenoma cases and CA in approximately 88% of the patients with macroadenoma.[16] The major blood vessels of giant PAs have been recently reported to originate from the branches of the infraclinoid portion of the ICA, such as the IHA.[13] In microadenomas receiving blood supply from the MHC and AFC at the time of development, the feeders are increased and changed during the growing process but no studies have been reported regarding the further stages and thereby the details remain unknown.

Conversely, it has been difficult to detect feeding arteries in PAs using flow void signals on MRI.[9,14] Okamoto *et al*. reported that only 4 of 134 (3.0%) PAs demonstrated flow void signals on T1WI.[14] These adenomas were large in size (32–60 mm) and nonfunctioning. Recently, a flow void signal was identified in 9 of 72 cases (12.5%) of PA on T2WI using 3.0 T MRI.[9] The size of tumors with a flow void signal was 30–58 mm. With the introduction of 3.0 T MRI, identification of a flow void signal was considered possible in a greater number of cases. Therefore, in this study, we aimed to carefully identify flow void signals using 3.0 T MRI in NFPAs. We identified flow void signals in 51 of 77 patients (66.2%) with NFPAs. As expected, the tumor size was significantly larger in tumors with a flow void signal compared with those without. However, we detected a flow void signal even in smaller NFPAs (minimum size: 20 mm). In addition, the flow void signal locations were divided into two groups (rostral and caudal).

Previously, we reported three blood supply patterns in NFPAs by TIC analysis using dynamic MRI. Interestingly, these patterns depended on tumor size. Tumor size in the ascending pattern group was significantly larger compared with the descending pattern group.

Furthermore, the flow void signal was more frequently observed in the ascending pattern group. Particularly, the

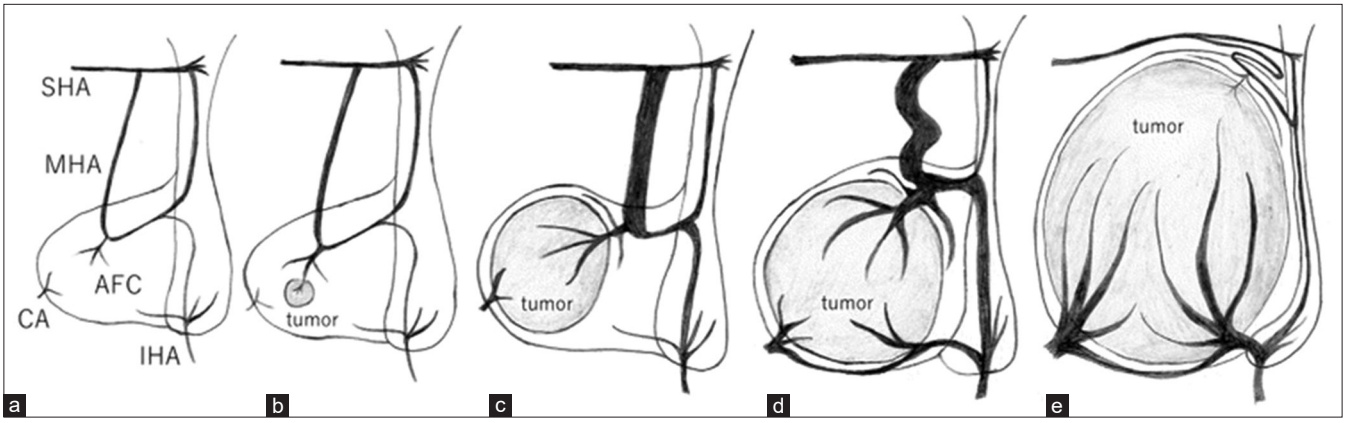

Figure 5: Illustration of the change in vascular supply associated with tumor growth. (a) The normal anterior lobe of pituitary gland mainly receives its arterial blood supply from the middle hypophyseal artery (MHA) and anterior fibrous core (AFC), which branch from the superior hypophyseal artery (SHA) and inferior hypophyseal artery (IHA). These vessels are anastomosed to each other. (b) A microadenoma occurring in the anterior lobe that receives blood supply from the MHA and AFC. (c) An early-stage pituitary adenoma (PA) receiving blood supply from the MHA and AFC. (d) The MHA tortured and the inferior hypophyseal artery (IHA) grown through anastomosis as the tumor enlarged. (e) When the large tumor compressed the normal anterior lobe of the pituitary gland, the MHA collapsed, and the IHA via AFC and capsular artery (CA) from the lower surface mainly perfused the PA.

flow void signal location in the ascending pattern group was more frequently on the caudal side. Conversely, the descending pattern was negatively associated with presence of a flow void. Moreover, there was a significant correlation in the presence of a flow void signal at the rostral side between the monophasic and ascending pattern groups.

From these results, we hypothesized that the pattern of feeding arteries might change in NFPAs as the tumor grows [Figure 5]. The main arteries, including the SHA and IHA strains, are anastomosed to each other. The vascular supply for microadenomas was mainly from the MHA and AFC, which originated from the SHA, similar to the feeding pattern in the healthy pituitary gland [Figures 5a and b]. MHA and AFC developed during the first stage of tumor growth [Figure 5c]. In this situation, the flow void signal was invisible or detected at the rostral side, and the TIC analysis showed a descending pattern. During the second stage, the IHA also developed with the anastomosis of the MHA and AFC [Figure 5d]. In such cases, flow void signals were detected at either or both sides (rostral and/or caudal), and the TIC showed a monophasic pattern. During the final stage, when the tumor grew large, its blood supply consisted primarily of the CA and IHA, with diminished blood flow from the MHA and AFC due to compression of the tumor [Figure 5e]. In such cases, flow void signals could be recognized at the caudal side, and the TIC revealed an ascending pattern.

Our results also suggest that the blood supply to PAs is complex and consists of a dense network of blood vessels; therefore, no cases showed a complete ascending or descending pattern.

The present study has some limitations. First, since NFPAs are generally fairly large at diagnosis, there were relatively small numbers of NFPAs with a descending pattern. Second, flow void signals were not confirmed as feeding arteries by other methods, such as DSA. Therefore, the findings of T2WI hypointensity which seemed to be flow void signals might include fibrous components such as emissary veins and septum. Further investigation is required to determine whether changes in hemodynamics during tumor growth can be observed in patients with NFPAs.

CONCLUSION

We successfully evaluated the blood supply pattern by TIC analysis and identified flow voids using 3.0 T MRI. The blood supply pattern was significantly associated with NFPA size. This suggests that the hemodynamics of NFPAs changes during tumor growth. As many variations in anastomosis exist, the blood supply pattern depends on the growth process of the tumor and development of each artery. However, our results could be useful for surgical planning and predicting tumor shrinkage after eTSS.

Acknowledgments

The authors are grateful to Ichiro Fujisawa for technical support and helpful comments on the manuscript. The authors thank Enago (https://www.enago.jp/) for the English language review.

Declaration of patient consent

Institutional Review Board (IRB) permission obtained for the study.

Financial support and sponsorship

JSPS KAKENHI (Grant Number 21K15820).

Conflicts of interest

There are no conflicts of interest.

REFERENCES

1. Adams JH, Daniel PM, Prichard MM. Some effects of transection of the pituitary stalk. Br Med J 1964;26:1619-25.
2. Baker HL. The angiographic delineation of the sellar and parasellar masses. Radiology 1972;104:67-78.
3. Bonneville JF, Cattin F, Gorczyca W, Hardy J. Pitutary microadenomas: Early enhancement with dynamic CT-implications of arterial blood supply and potential importance. J Radiology 1993;187:857-61.
4. Gorczyca W, Hardy J. Arterial supply of the human anterior pituitary gland. Neurosurgery 1987;20:369-78.
5. Gorczyca W, Hardy J. Microadenomas of the human pituitary and their vascularization. Neurosurgery 1988;22:1-6.
6. Harris FS, Rhoton AL. Anatomy of the cavernous sinus: A microsurgical study. J Neurosurg 1976;45:169-80.
7. Inoue T, Rhoton AL, Theele D, Barry ME. Surgical approaches to the cavernous sinus: A microsurgical study. Neurosurgery 1990;26:903-32.
8. Ito M, Kuge A, Matsuda K, Sato S, Kayama T, Sonoda Y. The likelihood of remnant nonfunctioning pituitary adenomas shrinking is associated with the lesion's blood supply pattern. World Neurosurg 2017;107:137-41.
9. Kurosaki M. Endonasal transsphenoidal surgery in department of neurosurgery, Tottori University. J Yonago Med Ass 2017;68:1-8.
10. Leclerco TA, Grisoli F. Arterial blood supply of the normal human pituitary gland. An anatomical study. J Neurosurg 1983;58:678-81.
11. Luschka H. Der Hirnanhang und die Steisdrüse des Menschen. Berlin: Verlag Von Georg Reimer; 1860.
12. McConnell EM. The arterial blood supply of the human hypophysis cerebri. Anat Rec 1953;115:175-203.
13. Ogawa Y, Sato K, Matsumoto Y, Tominaga T. Evaluation of fine feeding system and angioarchitecture of giant pituitary adenoma--implications for establishment of surgical strategy. World Neurosurg 2016;85:244-51.
14. Okamoto K, Ito I, Furusawa T, Sakai K. Intratumoral flow void in pituitary adenomas. Am J Roentgenol 1996;167:1070-1.
15. Parkinson D. A surgical approach to the cavernous portion of the carotid artery: Anatomical studies and case report. J Neurosurg 1965;23:474-83.
16. Powell DF, Baker HL, Laws ER. The primary angiographic findings in pituitary adenomas. Radiology 1974;110:589-95.
17. Sheehan HL, Stanfield JP. The pathogenesis of post-partnum necrosis of the anterior lobe of the pituitary gland. Acta Endocr 1961;37:479-510.
18. Stanfield JP. The blood supply of the human pituitary gland. J Anat 1960;94:257-73.
19. Xuereb GP, Prichard MM, Daniel PM. The arterial supply and venous drainage of the human hypophysis cerebri. Q J Exp Physiol 1954;39:199-21.

How to cite this article: Ito M, Mitobe Y, Hiraka T, Kanoto M, Sonoda Y. Changes in vascular supply pattern associated with growth of nonfunctioning pituitary adenomas. Surg Neurol Int 2022;13:481.